Rainfall, streamflow and sediment relationship in a hilly semi-agricultural catchment in Northern Italy

Article *in* Italian Journal of Agrometeorology · August 2014

5 authors, including:

Linda Pieri
University of Bologna

Francesca Ventura
University of Bologna

Miriam Hanuskova
Università degli Studi di Modena e Reggio Emilia

Rainfall, streamflow and sediment relationship in a hilly semi-agricultural catchment in Northern Italy

Linda Pieri[1,], Francesca Ventura[1], Marco Vignudelli[1], Miriam Hanuskova[2], Marco Bittelli[1]*

Abstract: *The paper analyzes the rainfall-flow relationships and the rainfall-flow-sediment relationships obtained respectively in two years and six months of monitoring in a small semi-agricultural catchment in the Apennines mountain range (Italy) with Mediterranean climate. The climate seasonality involves intra-annual variability in the hydrological response. Flow characteristics are correlated with rainfall depth, while duration, erosivity and previous rainfall are correlated with flow parameters depending on the season. The lack of a well defined relationship between these variables may be due to the flow mechanisms themselves, that vary with seasons. In summer Hortonian flow dominates, while in the other seasons runoff is generated by the Dunnian mechanism or by a combination of both mechanisms. Sediment concentration and soil loss are more correlated with streamflow than with rainfall parameters. Silt is the most eroded fractions. There is a significant correlation between the mean diameter of soil particles and the flow within the same flood event, but in general the relationship is influenced by supply condition (soil moisture, initial baseflow, etc).*
Keywords: *runoff, suspended sediments, Particle Size Distribution, Mediterranean climate, badlands.*

Riassunto: *Questo articolo riporta le relazioni pioggia-deflusso e pioggia-deflusso-sedimenti ottenute rispettivamente in due anni e sei mesi di monitoraggio in un piccolo bacino collinare negli Appennini, con clima mediterraneo. La stagionalità del clima determina una variabilità intra-annuale nella risposta idrologica. Il deflusso risulta essere ben correlato con la quantità di pioggia, mentre l'erosività (EI_{30}), la durata e la quantità di pioggia precedente hanno un coefficiente di correlazione variabile a seconda della stagione. La mancanza di una ben definita relazione durante tutto l'anno tra le variabili analizzate è probabilmente dovuta ai processi di generazione del ruscellamento superficiale che non sono costanti durante l'anno: in estate domina il meccanismo Hortoniano, mentre nelle altre stagioni il ruscellamento è generato dal meccanismo Dunniano o da una combinazione dei due. La concentrazione e la perdita dei sedimenti sono più correlate ai parametri del deflusso che a quelli della pioggia. Il limo è la frazione più erosa. Esiste una relazione significativa tra il diametro medio dei sedimenti e il flusso all'interno di un evento di piena, ma in generale la relazione è influenzata dalle condizioni al contorno (umidità del suolo, baseflow iniziale, ecc.).*
Parole chiave: *runoff, sedimenti sospesi, distribuzione diametro particelle, clima mediterraneo, calanchi.*

1. INTRODUCTION

One of the aims of hydrology is predicting the amount of flow that will occur from a given storm and the related sediment dynamics and transport. The hydrological response of a catchment derives from a combination of several factors: some of these are local, and can be considered characteristic of the catchment, such as geomorphology, soil texture, and land use; others are related to the rainfall characteristics, especially to those of the single precipitation event (Latron *et al.*, 2008) and to the antecedent conditions (soil moisture, land use, initial baseflow, etc; Gallart *et al.* 2005a), which are related to the area climate.

These issues are particularly relevant in Italy where erosion, that may be quite severe, occur very frequently (Cyr and Gramger, 2008; Conforti *et al.*, 2011; Borrelli and Shütt, 2014) and the seasonality of the Mediterranean climate, together with different kinds of vegetation coverage and land use, generate marked annual variations in the hydrology of the catchments (Soler *et al.*, 2008). López-Tarazón (2010) and Beven (2002) report that in these climates, rainfall-flow relationships is appreciable only during short wet periods of the year, while during the summer there is no linear relation. In addition, in the Mediterranean area other researches showed non-linear relation in the hydrological response of catchment at short (Piñol *et al.*, 1997) and long-term (>20 years; Gallart *et al.*, 2002; 2005a; 2005b; Latron *et al.*, 2008).

Moreover, quantitative information of rainfall impact on flow and suspended sediment features improve the predictive capability of catchment-scale models. In variable conditions, such as in region with a marked seasonal climate, relationships between parameters are complex (Garcia-Ruiz *et al.*, 2005). In these cases, the continuous monitoring of hydrology and sediment losses, together with a detailed elaboration of a high number of erosive rain events, can help understanding

*Corresponding author: linda.pieri2@unibo.it
[1] Department of Agricultural Science, University of Bologna, Bologna, Italy.
[2] Department of Engineering "Enzo Ferrari", University of Modena and Reggio Emilia, Modena, Italy.
Received 4 December 2013, accepted 9 March 2014.

the dynamic of flux of draining water bodies and erosion processes (Nu-Fang *et al.*, 2011; López-Tarazón *et al.*, 2010). Moreover the monitoring and the data processing at the event scale can provide information to understand which rainfall variables are the largest contributor of flow and soil loss, and their seasonality (López-Tarazón *et al.*, 2010; Nu-Fang *et al.*, 2011).

In addition, the particle size distribution (PSD) of the eroded sediments can provide useful information on the selective nature of the transport process (Heng *et al.*, 2011). This is fundamental to understand and simulate the transport of sediment and sediment-associated contaminants, including heavy metals, nutrients, micro-organics and radionuclides, in runoff and through river systems (Walling *et al.*, 1996).

The particle size composition of suspended sediment constitutes one of the most important physical properties of river sediment. Much of the suspended sediment load of a river is transported as composite particles or flocs (Walling *et al.*, 2000). A clear distinction should be drawn between the *in-situ* or effective PSD of the sediments (aggregates) and the ultimate particle size (Ongley *et al.*, 1981, Martinez-Mena *et al.*, 1998). The aggregates are important for understanding the soil transport and mobilisation (Walling *et al.*, 2000; Phillips and Walling, 1995), while information on the primary sediments helps to investigate on material fluxes, size-selective nature of sediment mobilization and sediment rates (Walling *et al.*, 2000).

Suspended sediment features depend on a high number of variables including the characteristics of the rainfall events and of the environment, such as soil type, topography of the area, and vegetation cover. Among these, there is no general agreement on which are the factors more affecting particles mobilization and transport. Some authors consider the original soil texture as the key point (Basic *et al.*, 2002; Young, 1980), while others identify the rainfall as a crucial variable, in particular its I_{30} (Martinez-Mena *et al.*, 1998) and kinetic energy (Miller and Baharuddin 1987; Nearing *et al.*, 2005; Parson and Stones, 2006).

The present study was undertaken against this background of uncertainties regarding the relations between rainfall – streamflow– quality and quantity of sediments, which still remains elusive. These relationships were examined in detail in a semi-agricultural hilly catchment, representative of the Apennines area, with Mediterranean climate. In particular, the objective of this study was to find relationships among rainfall, flow and sediment at event scale, starting from experimental measurements.

2. MATERIALS AND METHODS

2.1 The study area

The study was carried out in a hilly semi-agricultural catchment, 20 km from Bologna, in northern Italy (44°24' N, 11°28' E; Fig. 1). The climate classification is Mediterranean (Köppen-Geiger classification, Fig. 2), where the highest and lowest temperatures occur in July and December-January respectively, and the annual average precipitation (1992-2013) is 746 mm, concentrated in two rainy seasons, spring and fall. In summer short storms provide significant water input. Winter snowfalls are occasional and short-lived.

The 192 ha catchment has elevations ranging between 140 m and 350 m a.s.l, drained by the Centonara stream. Stream length is 1.5 km, with a mean slope of 8%. The hydrological trend of the Centonara stream is characterized by seasonal flow, showing often no-flow during the summer (Fig. 3).

The Centonara catchment shows a large heterogeneity from the point of view of lithology, geology, acclivity, and vegetation cover (Farabegoli *et al.*, 1994). As described by Farabegoli *et al.* (1994), the stratigraphy

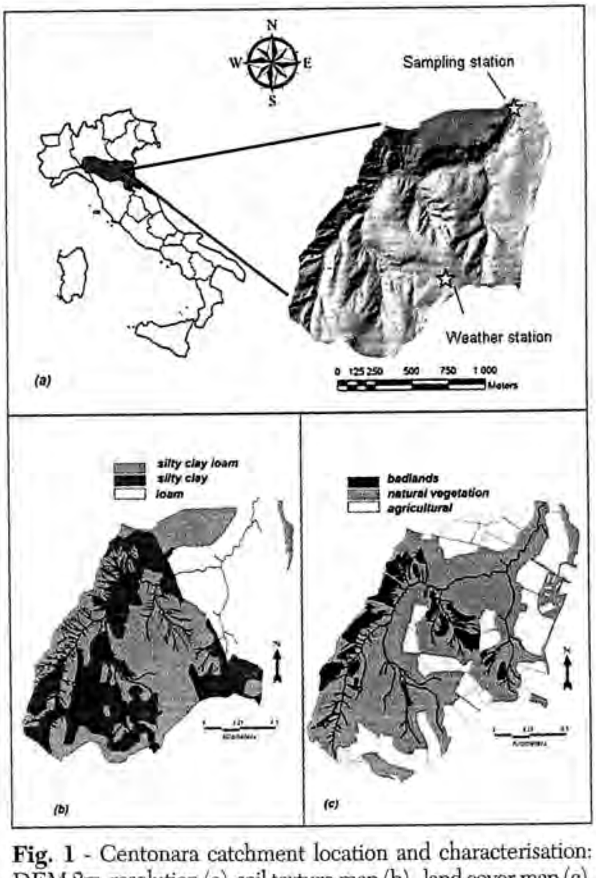

Fig. 1 - Centonara catchment location and characterisation: DEM 2m-resolution (a), soil texture map (b), land cover map (c).
Fig. 1 - Localizzazione e caratterizzazione del bacino del rio Centonara: DEM con risoluzione 2m (a), mappa della tessitura del suolo (b), mappa della copertura del suolo (c).

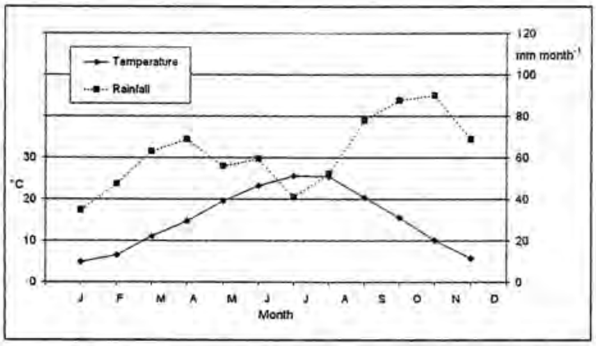

Fig. 2 - Bagnouls and Gaussen climo-diagram of the Centonara catchment (1992-2013).
Fig. 2 - Climogramma Bagnouls e Gaussen del bacino del Centonara (1992-2013).

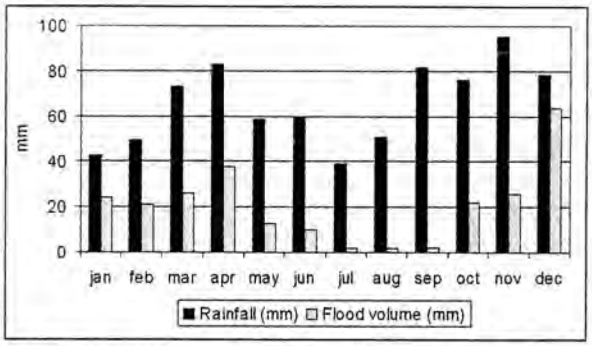

Fig. 3 - Monthly average rainfall and flow of the Centonara catchment of the period 1996-2009.
Fig. 3 - Medie mensili di pioggia e deflusso del bacino Centonara del periodo 1996-2009.

of the rock formations protruding from the oldest to the most recent is the following:

- The *Complesso caotico* (late Miocene – early Pliocene) is a various coloured sedimentary melange, including marl, marly-calcareous from older formations;
- Fam. Bismantova "Pantano" (Serravallino) witish silty marl.
- The *Pliocene intrappenninico* unit, yellowish grey sandstones and mudstones (Lower - Middle Pliocene): grey sandstones alternated with subordinated fine to medium grey marly clays;
- *Sabbie gialle di Imola* formation (Pleistocene): mainly composed by sandstones. Gravels and mudstones are also included;
- Terraced alluvial deposits (Middle-Upper Pleistocene): three orders of alluvial depositions.

According to Gardi (2001), five different soil units were identified and classified following Soil Taxonomy and FAO-UNESCO classification (Buol *et al.*, 1994). A description of the physical characteristics of these pedo-units is presented in Tab. 1.

Moreover, a sixth class was introduced to describe the badlands (*calanchi*) area. Badlands are land forms characterized by steep and bare lands, often subjected to accentuated erosion, land-sliding, mudflows, slope collapse and pipe development (Alexander, 1980; 1982). They are widely spread in the Apennine mountain chain (Battaglia *et al.*, 2003) and can be found in small hydrographical units, horse – shoe shaped. In Centonara catchment this formation is present in the steepest areas, determining formation of highly channelled erosion on steep terrains.

The superficial texture varies with the zone: it is loam in the flat area, while in the hilly part and the badlands area the textural classes are silty-clay-loam and silty-clay (Fig. 1b).

PEDO UNIT	Area [ha] [%]	Texture				CEC [meq/100g]	Organic matter [%]	Bulk density [g/cm^3]
		Classification	Sand [%]	Silt [%]	Clay [%]			
Sabbioni	53(28%)	Loam	49	35	16	19	1.3	1.54
Villa Massei	42(22%)	Silty-Clay-Loam	8	56	36	41	2.0	1.47
Villa Favorita	55 (29%)	Silty-Clay	7	47	46	33	1.4	1.48
Ca' Pivani	22 (11%)	Silty-Clay-Loam	5	59	36	33	4.7	1.40
Terrazzo G	6 (3%)	Silty-Clay-Loam	12	53	35	0	2.1	1.47
Calanchi	14 (7%)	Silty- Clay-Loam	13	54	33	-	-	-

Tab. 1 - Classification of pedo-units present in Centonara catchment, according to soil taxonomy and FAO/UNESCO classification. For each pedo-unit, area, texture, CEC, organic matter and bulk density of the superficial soil are reported.
Tab. 1 - Classificazione delle unità pedologiche presenti nel bacino del Centonara, in accordo con la classificazione tassonomica e la classificazione FAO/UNESCO. Per ciascuna pedo-unità sono riportate area, tessitura, CEC, sostanza organica e densità apparente del suolo superficiale.

As shown in Fig. 4, geomorphology presented a great variability in slope, ranging from less than 10% to more than 50%, with the intermediate classes, 20-30% and 30-35%, as predominant. Thus, the shape of the catchment has induced channelled erosion, highlighted by a dense network of small-size channels and, simultaneously, causing an irregular drainage pattern (Farabegoli, 1994).
During the monitored period, three land-use were present within the Centonara catchment: (I) arable lands, which were extended over 25% of the total area, prevalently in the flat fields, and cultivated mainly with alfalfa and cereals; (II) spontaneous vegetations (herbaceous, shrubs and trees), which occupied hilly fields with slope up to 40%, and riparian strips; (III) badlands, which were characterized by bare soil present on the most sloping area (over 40%) and represented about the 10% of the total area. A land-use map of the Centonara catchment is shown in Fig. 1c.

2.2 Flow and rainfall monitoring

At the catchment closure an automatic hydrological station (ISCO, 6700) was installed to measure the water flow of the Centonara stream and collect water samples to determine quantity and quality of sediments.
The stream bed, at the measuring point, was modified to have a trapezoidal shape of given dimensions, where the flow runs (Fig. 5).
An AV sensor use Doppler ultrasonic 500 KHz technology, which measures average velocity in the stream, and an integral pressure transducer, which measures liquid depths, were fixed at the bottom of the ditch. The level measurement ranged from 0.015 m to 3.05 m, showing the highly seasonal nature of the stream flow. Instrument resolution is 0.03 mm/d. The flux was computed as the product of water level, cross sectional area and water velocity. Samples were collected on time and volume base: one sample every 24h and every 3000 m^3 of flux, to follow both base flow

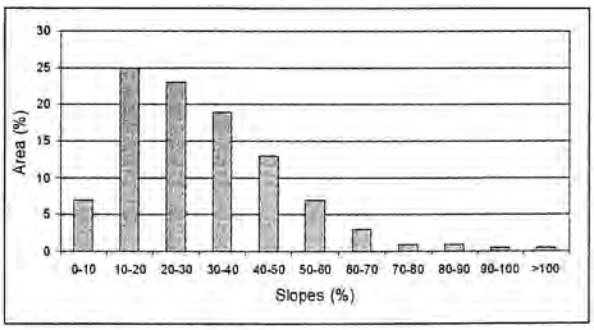

Fig. 4 - Histograms with the percentages for slope classes gathered with a 2m DEM.
Fig. 4 - Istrogramma con le percentuali per ciascuna classe di pendenza ottenute con DEM 2m.

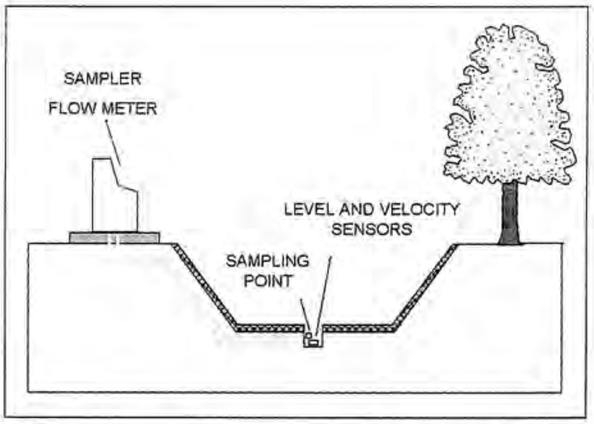

Fig. 5 - Stream cross section and equipment for flow measuring and sampling.
Fig. 5 - Sezione di misura del rio ed attrezzature per la misura e il campionamento del flusso.

and large events that could occur within a 24 h interval, and may transport the majority of sediments. Water samples were then analysed to determine sediment concentration (g/l) and their PSD.
Additionally, an automatic weather station within the catchment recorded rainfall every 10', air temperature, relative humidity, wind speed and direction, and solar radiation.

2.3 Data analysis

In this study two years, 2008 and 2009, were chosen to analyze rainfall, stream flow and suspended sediments data.
A total of 59 flood events were recorded in the period. A flood event is defined as a flow exceeding 1.5 times the baseflow at the beginning of the rainfall (as for López-Tarazón *et al.*, 2010; Nadal-Romero *et al.*, 2008; and Garcia-Ruiz *et al.*, 2005). For each hydrograph, baseflow and storm flow were separated using the program BFLOW.EXE, implemented by following the method proposed by Arnold and Allen (1999).
For each flood event, all relevant variables were measured or calculated. The rainfall associated with each flood event was characterized by: a) rainfall depth (R, mm), b) rainfall duration (D, h), c) mean rainfall intensity (Im, mm h^{-1}) d) maximum rainfall intensity over a 30-min period (I_{30}, mm h^{-1}), e) rainfall erosivity (EI_{30}, MJ mm $^{-1}$ha^{-1}h^{-1}, Wischmeier and Smith, 1978), f) amount of rain 1 day before (P1d, mm), and g) amount of rain in the 7 days before (P7d, mm).
The flow generated by the rainfall was described by a) flood volume (Q, m^3), b) baseflow at the beginning of the flood (Qb, $m^3 h^{-1}$), c) flood peak (Qp, m^3), d) flow coefficient (RC) calculated as the ratio between the runoff volume (after subtracting the baseflow) and the average rate of rainfall depth over a given event, and e)

stream power (Ω, W m^{-2}), i.e. the energy associated with flow per unit area for sheet flow. It was determined from the equation:

$$\Omega = \rho_w \; g \; S \; q_w \tag{1}$$

where ρ_w is the density of water (assumed to have a constant value of 1000 kg m^{-3}), g is the gravitational acceleration (9.81 ms^{-2}), S is the sine of the erosion surface slope and q_w is the volumetric flow ($m^3 m^{-2} s^{-1}$) per unit width of erosion surface (Proffitt and Rose, 1991). We used this parameter as a first rough approximation for stream power, since it assumes that surface flow is only determined by sheet flow. The sine of the erosion surface slope was obtained by computing the average slope of the whole catchment, by using the software ArcGIS. A better characterization of this parameter is obtained by using erosion models that account both for sheet and rill erosion as (Pieri *et al.*, 2014).
Sediments were described by the following characteristics: a) mean sediment concentration (SS g l^{-1}), b) maximum sediment concentration (SSm g l^{-1}), c) soil loss (TL, Mg), estimated multiplying flood volume (Q) and mean sediment concentration (SS), d) mean diameter (μ, mm), e) sediment texture (% clay, % silt, % sand), from the USDA classification. Sediment data were determined during flood events occurred in the period November 2008-April 2009.
Rainfall, streamflow and suspended sediment variables are listed in Tab. 2.

2.4 Particle size distribution analysis

Sediment concentration was determined by filtering flow samples and oven drying the filtrate at 105 °C. The particle size distribution (PSD) of the suspended sediments was referred to primary particles (i.e., sand, silt, clay) and it was obtained using the laser diffraction technique (LD). This analysis was performed with a small-angle light scattering apparatus (Malvern Master Sizer MS20, Malvern, England) equipped with a low-power (2 mW) Helium-Neon laser with a wavelength of 633 nm as the light source. Details for the pre-treatments of the samples and other apparatus characteristics are described in Pieri *et al.* (2006).
As previously demonstrated (Pieri *et al.*, 2006) the LD technique tends to underestimate the percentage of clay when compared to the sieve and pipette method, so the textural results were corrected using the equation of Eshel *et al.* (2004), y= 0.361x – 0.232, where x is the clay fraction determined by sieving and pipette and y is the clay fraction by LD. Since in our case we needed the clay fraction from sieving and pipette, having the fraction from LD, the equation was solved as y=(x+0.232)/0.361 where, in this case, x is the clay fraction from LD and y is the clay fraction by sieving and pipette. By applying this equation the obtained values were comparable to the textural fraction of the common soil databases.

2.5 Determination of the mean sediment diameter

The most eroded fraction was identified by determining the mean particle size diameter with the Gaussian model:

$$f(x) = [1/\sigma(2\pi)^{1/2}] \exp[-(x - \mu)^2/2\sigma^2 \tag{2}$$

where x is the particle diameter logarithm, μ is its mean and σ is the standard deviation, for a lognormal distribution. Since the PSD is represented by a cumulative curve, the integral form of Equation 2 for a Gaussian model was applied:

$$F(x) = 1/2 \{1 + \mathrm{erf}[(x - \mu)/\sigma\sqrt{2}]\} \quad \text{for } (x > \mu) \tag{3}$$

$$F(x) = 1/2 \{1 - \mathrm{erf}[(x - \mu)/\sigma\sqrt{2}]\} \quad \text{for } (x \le \mu) \tag{4}$$

Rainfall variables		Flow variables		Sediment variables	
R	Rainfall depth (mm)	Q	Flood volume (m^3)	SS	Mean sediment concentration (g l^{-1})
D	Rainfall duration (h)	Qb	Baseflow ($m^3 h^{-1}$)	SSm	Max sediment concentration (g l^{-1})
Im	Mean rainfall intensity (mm h^{-1})	Qp	Flood peak ($m^3 30'^{-1}$)	TL	Soil loss (Mg)
I_{30}	Max rainfall intensity over a 30-min period (mm h^{-1})	RC	Flow coefficient (mm mm^{-1})	μ	Mean sediment diameter (mm)
EI_{30}	Rainfall erosivity EI_{30} (MJ $mm^{-1} ha^{-1} h^{-1}$)	Ω	Stream power (Wm^{-2})	C	Clay fraction (%)
P1d	Previous rain 1 day before (mm)			Si	Silt fraction (%)
P7d	Previous rain 7 days before (mm)			Sa	Sand fraction (%)

Tab. 2 - Rainfall, flow and suspended sediment variables and associated abbreviation used in statistical analysis.
Tab. 2 - Variabili usate nell'analisi statistica ed associate abbreviazioni di pioggia, flusso e sedimenti sospesi.

where erf[ ] is the error function. The erf[ ] was computed by using the numerical approximation of Abramowitz and Stegun (1970):

$$erf(x) = 1 - (0.3480242T - 0.0958T^2 + 0.7478556T^3) \exp(-x^2) \quad (5)$$

where $T = 1/(1 + 0.47047x)$.

The approximation of the error function as described in Equation 5, was tested by computing values of T, which ranged from 0.34 to 0.99 for $F_1(x)$ and from 0.266 to 0.99 for $F_2(x)$. These values provided a satisfying approximation of the error function (Abramowitz and Stegun, 1970). Since the PSD distribution of the sediments showed a unimodal behaviour, a unimodal model was tested to calculate the mean and standard deviation. The model was fit to experimental PSD data by using a non-linear least square fitting procedure (Marquardt, 1963), with μ and σ as fitting parameters.

2.6 Statistical analysis

To assess the relationship between variables, a linear regression by Pearson matrix (Warner, 2012) was used. The Pearson product-moment correlation coefficient is a measure of the strength of the linear relationship between two variables. If the relationship between the variables is not linear, the correlation coefficient does not adequately represent the strength of the relationship between the variables.

3. RESULTS AND DISCUSSION

3.1 General description of rainfall and flood events

During the two years of study period a total of 206 rainfall events were recorded, with a total yearly amount of 795 mm in 2008 and 803 mm in 2009. The events majority were mild and short-lived and did not produce an increase in the flow of Centonara compared to baseflow. Only 59 rain events produced a peak of flow. Among these 21 occurred in spring, 18 in fall, 15 in winter, and 5 in summer. Tab. 3 summarizes the general characteristics (maximum, minimum, mean values and standard deviation) of the 59 rainfall events and the associated observed floods:

- the minimum rainfall (R) for a single event generating a peak flow was 4.6 mm (17 June 2008 and 28 December 2009), the maximum 75.8 mm (12 November 2008), the mean 18.2 mm; the 59% was greater than 10 mm, amount of daily rainfall that can be assumed as threshold for flow start in semiarid environment (Boardman *et al.*, 2003; Piccarreta *et al.*, 2006).
- the duration of events (D) varied between 0.3 and 61 h, with a mean value of 15.4 h; 29 events showed duration shorter than 13 h (value at the 50° percentile); the shortest events occurred in summer, with a mean of 5.4 h.
- the maximum 30-min rainfall intensity (I_{30}) ranged between 1.6 and 48.3 mm h^{-1}, with a mean of 8.3 mm h^{-1}. These values showed that most of the rainfalls had relatively low intensity: only 4 events (7%) exceeded 20 mm h^{-1}, which is the minimum estimated value to consider the infiltration excess surface flow as "Hortonian overland flow" (Selby, 1982);
- the erosive index (EI_{30}) ranged between 1 and 331 MJ mm $ha^{-1}h^{-1}$, with a mean value of 35 MJ mm $ha^{-1}h^{-1}$. The two events with EI_{30} >300 MJ mm $ha^{-1}h^{-1}$ occurred both in summer (5 July 2009 and 28 august 2009).
- P1d and P7d were very variable ranging from 0 to 33.6 and 87.8 mm, respectively.

The rainfall events reflected the typical characteristics of Mediterranean climate. During the summer there

Parameter	*Minimum*	*Maximum*	*Mean*	*St. dev.*
R (mm)	4.6	75.8	18.2	14.9
D (h)	0.3	61.0	15.4	12.9
Im (mm h^{-1})	0.2	35.4	3.0	6.6
I_{30} (mm h^{-1})	1.6	48.3	8.3	8.6
EI_{30} (Mjmm^{-1}ha^{-1}h^{-1})	1	331	35	65.3
P1d (mm)	0	33.6	4.8	8.2
P7d (mm)	0	87.8	33.3	20.6
Q (m^3)	0	91251	18581	2030
Qb (m^3 h^{-1})	0	468	137	132
Qp (m^3 $30'^{-1}$)	3.3	8130	1579	2030
RC (mm mm^{-1})	0.0	2.6	0.5	0.5
Ω (W m^{-2})	3	12000	2000	2864

Tab. 3 - General description of the flood events analysed in the paper.
Tab. 3 - Descrizione generale degli eventi di piena analizzati nell'articolo.

were the least numerous but most potentially erosive events: they had the highest average values of I_{30} (I_{30} = 22.6 mm h^{-1}) and EI_{30} (EI_{30}=140 MJ mm $ha^{-1}h^{-1}$). The mean P1d and P7d were 0.2 and 21.7 mm, respectively, while in the rest of the year mean P1d ranged between 4.9 and 5.6 mm and mean P7d between 28.6 and 38.1 mm.

The comparison between the two rainy seasons indicates that the fall events were the longest (mean D=21 h), but they were less intense than the spring events (mean I_{30}= 9.4 mm h^{-1} in spring, 6.8 mm h^{-1} in fall). Finally, the winter events were long (mean D=15.2 h), but with very low intensity (mean I_{30}=3.3 mm h^{-1}).

The main characteristics of the flood events originated from the 59 rainfall events were:

- the flow had a seasonal pattern more pronounced than the precipitation: the flood volume of single event was minimum during the driest period (summer and the beginning of fall) and maximum in correspondence of strong rainfall events. Its value ranged (not considering 0) between 13 and 91251 m^3, occurred on July, 21, 2008 and March, 30, 2009, respectively, while the mean was 18581 m^3. The peak flow ranged between 3.3 and 8230 m^3 $30'^{-1}$, with a mean value of 1579 m^3 $30'^{-1}$. The initial baseflow was always lower than 468 m^3 h^{-1}, and 0 during the driest period. During the dry period, some flux events occurred, in correspondence of heavy storm events. In this period the maximum flood volume was 333m^3, with a peak of 52 m^3 $30'^{-1}$.
- the stream power had a trend similar to the flood volume. Its value ranged between 3 W km^{-1} and 12000 W m^{-2}, with a mean of 2000 W m^{-2}.
- the flow coefficient ranged from 0.002 to 2.560. Looking at the seasonality the mean RC was 0.540, 0.002, 0.300, 0.790, respectively in spring, summer, fall, and winter. This means that in winter nearly 80% of the precipitation turned into flow, whereas during the summer it was less than 1%.

Fig. 6 shows the daily rainfall and flood volume in these two investigated years. The figure highlights that the maximum flux occurred in winter, while in the period July-October the stream was dry, apart from few small flood events occurred in 2008 during particularly intense summer storms. At the end of the dry-spell, each rain event (or series of rain events) greater than 5 mm generated a peak flow.

3.2 Relation between rainfall and flow at event scale

Once both rainfall and flow characteristics were analysed, data were elaborated with the Pearson correlation matrix (Tab. 4). Considering all flood events, rainfall quantity, R, and duration, D, were significantly

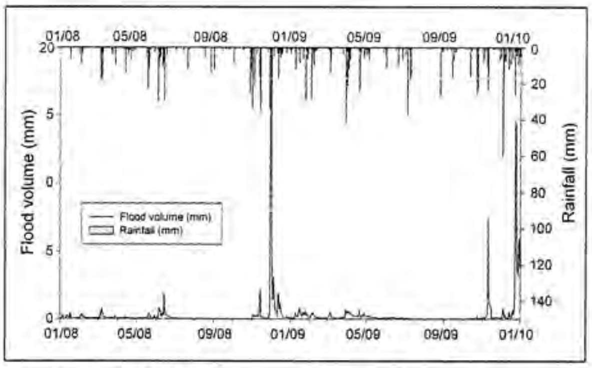

Fig. 6 -Daily flood volume and rainfall during the two years 2008 and 2009.

Fig. 6 - Dati giornalieri di flusso e pioggia degli anni 2008 e 2009.

correlated (P<0.05) with flow, Q (0.58, 0.57). On the other hand, no significant relations were found between all the flow variables with both the rainfall intensity factors (I_{30}, Im, EI_{30}) and the catchment moisture condition (P1d and P7d).

If the Pearson matrix is calculated without the dry period when the baseflow is zero, the statistical indexes greatly improve: rainfall quantity, R, resulted to be correlated with flow Q (0.81), peak of flow Qp (0.57), and stream power Ω (0.56) (data not shown). Moreover, considering these events, there was a direct relationship between the amount of rainfall and the flow depth (Fig. 7). Similar linear relation was found in comparable catchments (Nadal-Romero *et al.*, 2008; López-Tarazón *et al.*, 2010), suggesting that the amount of precipitation seems to be the dominant parameter of the precipitation event, strongly influencing the hydrological response: the larger the precipitation event (considering both depth and duration), the larger the resultant floods, in term of flow depth and peak.

Considering the strong seasonality of the rainfall and flow pattern (in Fig. 3 the monthly distribution), the events were divided seasonally and the Pearson correlation for each group was repeated. The significant relationships obtained with the new arrangement are summarised in Tab. 5. R and EI_{30} were the only rainfall parameters always correlated with the flux, independently from the season. In particular rainfall depth, R, was the parameter better linked to flood volume (Q), flood peak (Qp) and stream power (Ω).

During the rainy seasons (fall and spring), the rainfall parameters related to the flow were the same: in addition to R and EI_{30}, D and P7d were significant. Winter is the poorest of significant correlations: a part from R and EI_{30}, mean intensity (Im) was correlated both with flood peak (Qp) and stream power (Ω). Summer is the season with the best and most numerous correlations: the maximum intensity (I_{30}) assumed a key

	R	D	Im	I_{30}	EI_{30}	P1d	P7d	Q	Qp	Qb	RC	Ω
R Rainfall depth	1											
D Rainfall duration	0.63	1										
Im Mean rainfall intensity	0.00	-0.34	1									
I_{30} Max rainfall intensity	0.34	-0.19	0.66	1								
EI_{30} Rainfall erosivity	0.54	0.05	0.50	0.91	1							
P1d Prec rain 1 day before	-0.04	-0.06	-0.10	-0.06	-0.13	1						
P7d Prec rain 7 days before	0.18	-0.04	0.03	0.02	0.04	0.23	1					
Q Flood volume	**0.58**	**0.57**	-0.17	-0.05	0.07	0.08	0.30	1				
Qp Flood Peak	**0.50**	0.31	-0.12	0.15	0.21	0.16	0.29	0.76	1			
Qb Baseflow	-0.12	0.22	0.03	-0.20	-0.18	-0.01	0.13	0.29	0.22	1		
RC Flow coefficient	0.11	0.25	-0.20	-0.18	-0.15	0.34	0.33	0.73	0.66	0.38	1	
Ω Stream power	0.40	0.26	-0.14	0.01	0.05	0.23	0.37	0.87	0.86	0.28	0.79	1

Tab. 4 - Pearson matrix correlation between rainfall and flow variables of all the flood events (n=59). In bold the significative correlation between rainfall and flow variables (0.05 level).
Tab. 4 - Matrice di correlazione di Pearson tra le variabili di pioggia e flusso di tutti gli eventi di piena studiati (n=59). In grassetto le correlazioni significative tra le variabili di pioggia e flusso (livello 0.05).

role, because of its high correlation with flood peak (Qp) and stream power (Ω). This was due to stormy rainfall events, characterized by short duration and high intensity.
The seasonal Pearson matrices also evidenced the importance of the hydrological conditions in the period before the flow events (P7d). Apart for the winter, in all the seasons P7d is correlated with the flow, especially in relation to the baseflow.
These different relationships could be explained considering the mechanisms of runoff generation and thus of the streamflow, related to the seasonality of the Mediterranean climate of the investigated area.
The principal mechanisms of runoff generation are two: the Dunnian and the Hortonian mechanisms (Dunne, 1978; Freeze, 1971). The first is typical of areas with humid climate and vegetated coverage, and is caused by the saturation of the surface layers for the raising of the water table, due to the combined contribution of

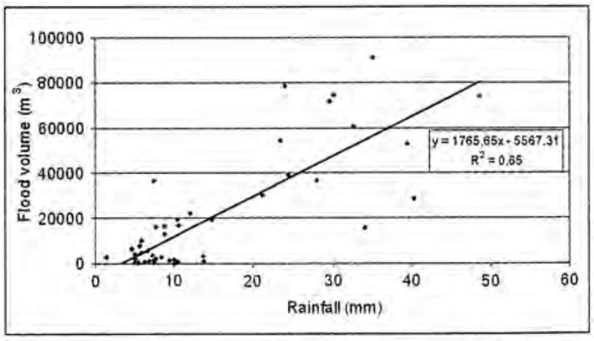

Fig. 7 - Event-scale correlation between rainfall and flow (in the plot the dry period is not considered).
Fig. 7 - Correlazione tra pioggia e flusso a scala di evento (nel grafico il periodo secco non è considerato).

subsurface runoff and precipitation. In this case the flow is formed by two components surface and subsurface runoff, the latter determines the expansion and contraction of the saturation area.
The Hortonian mechanism explains the origin of runoff when the precipitation rate exceeds the infiltration capacity (Horton, 1933). This mechanism is typical of arid or semi-arid climates while it is rare with humid climate characterized by deep and greatly permeable soils.
Even if we did not directly measure the mechanism of runoff generation in the Centonara catchment we can use scientific literature to try to describe the processes. As reported by Bittelli *et al.* (2011), in Mediterranean regions characterized by hot and dry summer, similar to the semi-arid regions, and cold and humid winter, similar to continental regions, runoff is generated by both the mechanisms, Hortonian and Dunnian, which can occur separately or simultaneously on different areas of the catchment. Their occurrence depends mainly on topographical features and on the season and therefore it may not be possible to hydrologically classify a catchment as solely Hortonian and Dunnian, but a catchment can present both mechanisms. This complex process is described in several catchments of the Mediterranean area (Bittelli, 2011; Latron *et al.*, 2008; Soler *et al.*, 2008; Nadal-Romero, 2008; Lana-Renault and Regüés, 2009; López-Tarazón, 2010) and could help to understand the correlation results.
Considering the prevalence of vertisoils of the Centonara catchment, and the results of the study reported by Bittelli *et al.* (2011) in a similar Apennines catchment, it is plausible that in summer the runoff in

Fall	Winter	Spring	Summer
R vs Q (0.64) R vs Qp (0.74) R vs Ω (0.55)	R vs Q (0.88) R vs Qp (0.80) R vs RC (0.57) R vs Ω (0.80)	R vs Q (0.83) R vs Qp (0.68) R vs Ω (0.60)	R vs Q (0.90) R vs Qp (0.96) R vs Qb (0.86) R vs RC (0.72) R vs Ω (0.90)
EI_{30} vs Qp (0.57)	EI_{30} vs Qp (0.80) EI_{30} vs Ω (0.63)	EI_{30} vs Qp (0.73) EI_{30} vs Ω (0.56)	EI_{30} vs Q (0.71) EI_{30} vs Qp (0.85) EI_{30} vs Qb (0.64) EI_{30} vs RC (0.56) EI_{30} vs Ω (0.99)
D vs Q (0.64) D vs Qp (0.64) D vs Qb (0.53) D vs RC (0.54) D vs Ω (0.50)		D vs Q (0.68)	D vs Ω (-0.73)
P7d vs Q (0.51) P7d vs Ω (0.61)		P7d vs Qb (0.51)	P7d vs Q (0.87) P7d vs Qp (0.94) P7d vs Qb (0.85) P7d vs RC (0.67) P7d vs Ω (0.87)
	Im vs Qp (0.61) Im vs Ω (0.66)		Im vs Ω (0.72)
			Imax vs Q (0.54) Imax vs Qp (0.70) Imax vs Ω (0.95)

Tab. 5 - Significative Pearson matrix correlations of all the studied events divided for seasons. In parenthesis the correlation coefficient.

Tab. 5 - Correlazioni di matrice di Pearson significative di tutti gli eventi studiati suddivisi per stagioni. In parentesi il coefficiente di correlazione.

slope areas is mainly generated by the Hortonian mechanism. This simplify the relationship between rainfall and flow variables and better explain the correlation coefficients. Moreover, in this season the previous rainfall (P7d) assumes a strong role in the hydrological response of the catchment. In fact, the previous cumulative rainfall determines the saturation of the first layer of soil, facilitating the generation of surface runoff.

Probably in the rest of the year, runoff is generated by a mix of the Dunnian and Hortonian mechanisms. Moreover, in wet seasons and with vegetation, soil is already totally or partially saturated and the flow may occur after a new rain, even if small (the limit is about 5mm), because of the soil water content conditions. Indeed, as shown by Morbidelli *et al.* (2012), the antecedent soil water content is a crucial element in determining the surface runoff hydrograph and its knowledge is very important when distributed models for the estimate of basin response to rainfall have to be formulated.

As reported in Pieri *et al.*, 2014, in Centonara catchment badlands and/or impervious areas constitute the most relevant flow sources. Probably during the summer, in these areas, intense storms fall on dry soil and produce only ephemeral floods, while the vegetated areas generate few runoff, because the infiltration is the dominant process. After the dry season, gradually the Centonara stream begins to fill with water (Fig. 3), thanks to rainfall events that recharge ground water and soil water content, also producing local perched aquifers. In this period there is a dominance of saturated excess flow process (Lana-Renault, 2009) and the Dunnian mechanism is usually predominant.

3.3 Eroded sediment quantity as a function of hydrological variables

Sediments, collected during the period from November 2008 to April 2009, were analyzed in relation to rainfall and flow by means of the Pearson correlation.

The quantity analysis highlighted that the soil loss per event was very variable and ranged between 0.04 t to 0.80 t, recorded on April, 4, 2009 and March, 31, 2009, respectively. The Pearson matrix in Tab. 6 shows correlations between rainfall, flow and sediment variables. The soil loss, TL, was well correlated with flood peak, Qp, (0.65) and stream power, (Ω) (0.73). No correlation was found between rainfall variables and the soil loss (TL). The sediment concentration, SS, were significantly correlated with the flow coefficient, RC, (0.59) and with the flood volume, Q (0.55).

For flood events higher than 3000 m^3 the automatic sampler provided till to four samples depending on the flood event, allowing a more detailed analysis of the event and adding the measure of the maximum concentration of the event (SSm). For these specific events the Pearson analysis (data not shown) highlighted good correlations between SSm and most of the rainfall characteristics (R (1.0), D (0.92), I_{30} (0.95), EI_{30} (0.91), P1d (0.79)) and of flux (Qp (0.72), Qb (-0.79), RC (-0.58)). The flow variables resulted to be the most relevant factors in controlling the sediment loss and the mean concentration, while rainfall variables assumed a key role in the determination of the maximum sediment concentration. These results are clearly showing that rainfall amounts are not sufficient to perform a correct analysis of sediment transport, but geomorphological and soil information are needed.

3.4 Particle Size Distribution of eroded sediment

As an example, the PSD density and cumulative curve for the eroded sediment collected at the outlet point of the catchment during a representative flood event is shown in Fig. 8. The plot shows the experimental data (dots) and the fitted Gaussian model (solid line) obtained with the Equation 2. The observed data were all well represented by the Gaussian model, as the RMSE was always < 0.03.

The LD analyses of the eroded sediment showed that PSD had an unimodal distribution and the silt fraction was the most represented: the mean value (μ), obtained from the Gaussian model, ranged from 4.2 to 100.6 μm with a standard deviation (σ) varying from 1.49 to 2.51 (apart from 43.34 recorded on January, 25, 2009).

The results of the PSD were then subdivided in the USDA textural classes. Since the analysis of the PSD with the LD technique, as previously demonstrated (Eshel *et al.*, 2004; Pieri *et al.*, 2006), when compared with the pipette technique, tends to underestimate clay, the conversion equation of Eshel *et al.* (2004) was apply on the data. The term *underestimate* is used here simply because the pipette measurement is a classic and old methods, however it is not given that it provides

	R	D	Im	I_{30}	EI_{30}	P1d	P7d	Q	Qp	Qb	RC	Ω	μ	C	Si	Sa	SS	TL
R Rainfall depth	1																	
D Rainfall duration	0.92	1																
Im Mean intensity	-0.20	-0.46	1															
I_{30} Max intensity	0.91	0.84	-0.02	1														
EI_{30} Erosivity	0.90	0.84	-0.14	0.97	1													
P1d Prev rainfall 1 day	-0.37	-0.31	-0.27	-0.32	-0.25	1												
P7d Prev rainfall 7 days	-0.45	-0.36	0.48	-0.23	-0.38	0.04	1											
Q Flood volume	0.46	0.53	-0.24	0.20	0.12	-0.26	-0.10	1										
Qp Flood Peak	0.78	0.66	0.01	0.59	0.52	-0.37	-0.40	0.76	1									
Qb Baseflow	-0.39	-0.27	0.20	-0.27	-0.29	-0.08	0.51	0.08	-0.29	1								
RC Flow coefficient	-0.37	-0.21	-0.22	-0.51	-0.54	0.32	0.16	0.57	0.05	0.34	1							
Ω Stream power	0.09	0.01	0.15	-0.15	-0.20	-0.11	-0.02	0.78	0.55	0.16	0.72	1						
μ Mean diameter	-0.08	-0.14	-0.17	-0.40	-0.31	-0.23	-0.21	0.16	-0.06	-0.21	0.16	0.35	1					
C % clay	0.16	0.04	0.40	0.22	0.17	0.13	0.18	0.42	0.41	0.43	0.42	**0.63**	-0.36	1				
Si % silt	0.03	0.13	0.02	0.34	0.28	0.15	0.14	-0.40	-0.13	0.01	-0.43	**-0.70**	-0.89	-0.11	1			
Sa % sand	-0.10	-0.27	0.01	-0.39	-0.28	-0.15	-0.31	0.06	-0.02	-0.20	0.12	0.42	0.93	-0.16	-0.90	1		
SS Mean sed conc	0.22	0.41	-0.32	0.27	0.21	0.37	0.11	**0.55**	0.32	0.18	**0.59**	0.34	-0.49	0.57	0.21	-0.55	1	
TL Soil loss	0.30	0.43	-0.26	0.09	0.01	-0.09	0.01	**0.96**	**0.65**	0.22	**0.69**	**0.73**	-0.02	0.48	-0.24	-0.13	0.69	1

Tab. 6 - Pearson matrix to evaluate correlation between eroded sediments and hydrological variables. In bold the significative correlation between rainfall, flow and sediments variables (0.05 level).

Tab. 6 - Matrice di Pearson per valutare la correlazione tra i sedimenti erosi e le variabili ideologiche. In grassetto le correlazioni significative tra le variabili di pioggia, flusso e sedimenti (livello 0.05).

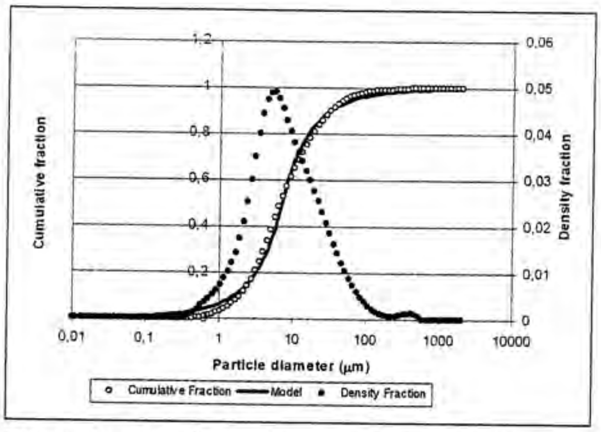

Fig. 8 - Density and cumulative distribution of soil fractions for a representative sediment sample. Dot are experimental data, solid lines are modeled thought the Gaussian model.
Fig. 8 - Distribuzione di densità e cumulativa delle frazioni del suolo di un campione di sedimento rappresentativo. I punti sono dati sperimentali, mentre la linea rappresenta il fitting ottenuto con il modello gaussiano.

more accurate results with respect to laser diffraction. Our conversion was performed simply to compare current results with common soil databases.

Results showed that suspended sediments were on average 49% of silt, 27% of clay and 24% of sand. These results confirm the selective nature of the transport process with respect to the silt diameter particles and are in accordance with Young (1980) which affirms that soil particles belonging to this fraction are the easiest particles to transport.

It is important to stress that the PSD analysis was carried out on ultimate particles (sand, silt and clay). As shown in Fig. 9 the dispersion action to destroy the particles aggregates affect the PSD analysis. Fig. 9

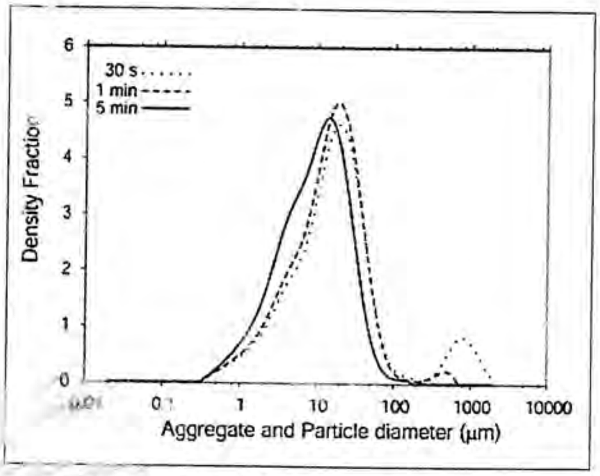

Fig. 9 - Example of PSD of suspended sediment aggregated and dispersed with ultrasonic waves at diverse time.
Fig. 9 - Esempio di PSD di sedimenti sospesi aggregati e dispersi attraverso onde ultrasoniche di diversa durata.

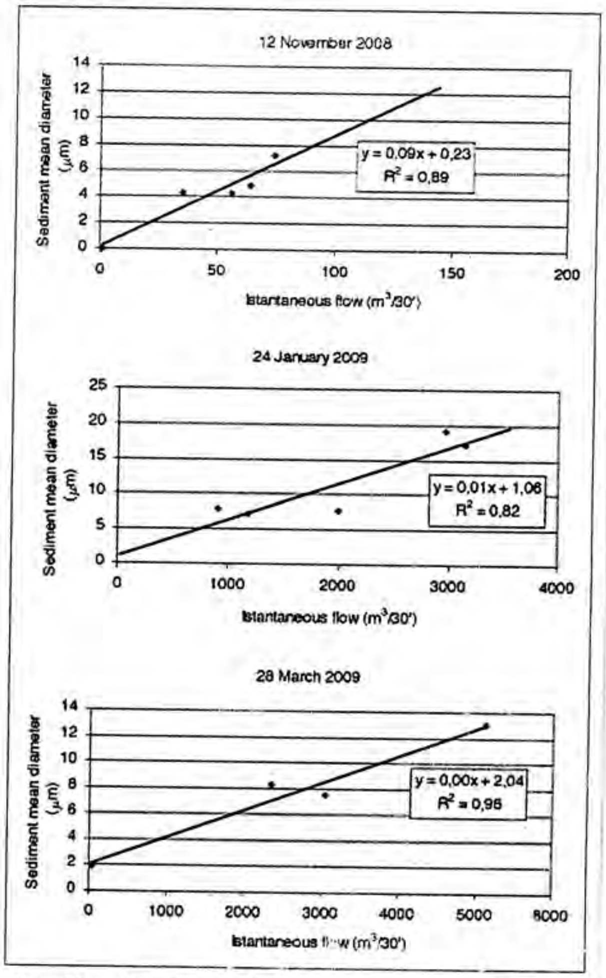

Fig. 10 - Correlation between instantaneous flow and sediment mean diameter for 3 events recorded in 2008-2009, during the seasons fall, winter and spring.
Fig. 10 - Correlazione tra flusso istantaneo e media del diametro del sedimento per 3 eventi registrati nel 2008-2009 durante le stagioni autunno, inverno e primavera.

displays an example of sediment PSD, obtained with samples subjected to increasing time of ultrasound waves. The dot line represents the sample subjected to 30 seconds to ultrasound waves. When the treatment is short and aggregates had no time to be dispersed, the distribution presents two modes, a large one around 10 μm and an other smaller around 1000 μm. As the time of treatment with ultrasound waves increases (from 1 min to 5 min), the sample is dispersed until it is formed only by ultimate particles. The solid line represents the sediment PSD, when the sample is totally dispersed: the mode around 1000 μm disappeared and the main mode is slightly shifted toward smaller diameters. This confirms that the clay particles are detached and transported in form of aggregates and only if subjected to dispersion are reduced in primary particles.

3.5 Suspended sediment quality as a function of hydrological variables

As described above, the mean diameter (μ) of the suspended sediments is not constant for all flood events and it may depend on the flow and rainfall features. The sediment PSD results were analysed with the Pearson matrix to emphasize relationships with rainfall and flow variables.

There was a significant correlation between the stream power (Ω) and the textural fraction percentages, especially with silt (-0.70) and clay (0.63) (Tab. 6), meaning that an increase of stream power leads to a decrease in the mean diameter of the suspended sediments. This is realistic considering that, as previously shown, the particles are often transported in aggregates form and the stream power can break the aggregates.

Looking at single flood event, the sediment mean diameter (μ) was plotted as a function of instantaneous flow, which means the flow recorded during the water and sediment sampling. In Fig. 10, flood events occurred in three different seasons (spring, fall and winter) were presented: even if data were very different, all the correlation were significant (R^2> 0.81). Instead, considering all the data collected during these events together, the relationship is not significant. According to Walling (2000), the lack of a well-defined correlation between flood volume and sediment mean diameter highlights that the remobilization of coarse channel bed sediment as flow velocity and shear stress increase. It is not always true, as assumed by traditional hydraulics theories, that an increase in flux, and therefore of shear stress and turbulence, determine the transport of particles with larger diameters: in previous studies researches report of sediment that remains essentially constant or becomes coarser or finer as flow increases (Walling and Moorehead, 1989; Walling *et al.*, 2000). Therefore, there is a direct and significant correlation between the mean diameter and the flux within the same event of flood, but in general the trend of this relationship varies with the site condition. The seasonal and storm-period variation in catchment condition, the spatial variability of rainfall and evapotranspiration and the soil heterogeneity (geology, acclivity and land use) influence the supply condition. These produce various initial conditions such as soil moisture and initial baseflow, that influence the process and fail to reach a generalized behavior.

4. CONCLUSION

Quantitative information of rainfall impact on flow and suspended sediment features would improve the predictive capability of catchment-scale models. Research on soil losses in catchment draining highly erodible materials (e.g. badlands and soft materials) is of increasing interest to provide detailed data for model calibration and validation in active geomorphic environment, together with the concern for management purposes. Results of the present study confirm the complexity of the hydrological and erosive response to rainfall events in a small but heterogeneous hilly catchment. Since the Mediterranean region are characterized by a strong seasonality a possible approach to the study is working on the relation rainfall-flow at season-base. The flow in fact depends on the runoff generation, which is originated differently during the year: in summer runoff is prevalently generated by the Hortonian mechanism, while in the other periods by the Dunnian mechanism or a combination of the two mechanisms. However, to assess these complex phenomena, physically-based models are still the best solution, since they can describe the surface runoff-infiltration-redistribution phenomena in a quantitative way (Bittelli *et al.*, 2011), and therefore correctly discriminate between different hydrological processes. The statistical analysis evidenced that the amount of precipitation is the dominant parameter: significant correlations were obtained between rainfall quantity and duration with flow, and not with rainfall intensity factors and catchment moisture condition.

Working at season-base more significant correlation were found and rainfall and erosivity became the key parameters. In rainy seasons (fall and spring) flow depended on rainfall duration and depth, and EI_{30}. In winter the significant correlations were between rainfall depth, EI_{30}, and rainfall mean intensity with flow peak and stream power. During the summer the maximum intensity (I_{30}) assumed a key role, showing a high correlation with peak flood (Qp) and stream power (Ω). The Pearson matrices also evidenced the importance of the hydrological conditions in the period before the flow events (P7d). Apart for the winter, in all the seasons P7d is correlated with the flow, especially in relation to the baseflow.

The sediment data analysis highlighted the lack of a well-defined correlation with flow. There is not a simple function of transport capacity or flow hydraulics. There is a direct and significant correlation between the mean diameter and the flux within the same event, but in general this relationship varies with the supply conditions, such as the spatial variation due to the soil heterogeneity (geology, acclivity and land use), the soil moisture and the initial baseflow, that influence the process and fail to reach a generalized response.

ACKNOWLEDGMENTS

We thank Marco Martorana for his help with the PSD analysis and Prof. Paola Rossi for her collaboration to the research.

REFERENCES

Abramowitz M., Stegun I.A., 1970. Handbook of Mathematical Functions. Dover Publications, New York.

Alexander D., 1980. I calanchi accelerated erosion in Italy. Geography, 65, 95-100.

Alexander D., 1982. Difference between "calanchi" and "biancane" badlands in Italy. In: Bryan, R., Yair, A. (Eds.), Badland Geomorphology and Piping. GeoBooks, Norwich, pp. 71-88.

Arnold J.G., Allen P.M., 1999. Automated methods for estimating baseflow and ground water recharge from streamflow records. Journal of the American Water Resources Association, 35, 411-424.

Basic F., Kisic I., Nestroy O., Mesic M., Butorac A., 2002. Particle size distribution (texture) of eroded soil material. J. Agron. Crop Sci., 188, 311-322.

Battaglia S., Leoni L., Sartori F., 2003. Mineralogical and grain size composition of clays developing calanchi and biancane erosional landforms. Geomorphology, 49, 153-170.

Beven K., 2002. Flow generation in semi-arid areas. In: Bull, L.J., Kirkby, M.J. (Eds.), Dryland Rivers. Jhon Wiley & Sons, Chichester, pp. 57-105.

Bittelli M., Pistocchi A., Tomei F., Roggero P.P, Orsini R., Toderi M., Antolini G., Flury. M., 2011. Criteria-3D: a mechanistic model for surface and subsurface hydrology for small catchments. In book: Soil Hydrology, Land Use and Agriculture. Publisher: Cabi Publishing, Editors: Manoj K. Shukla, pp. 13.

Borrelli P. and Shütt B., 2014. assessment of soil erosion sensitivity and post-timber-harvesting erosion response in a mountain environmental of central Italy. Geomorphology, 204, 412-424.

Broadman J., Parsons A.J., Holland R., Holmes P.J., Washington R., 2003. development of badlands and gullies in the Sneeuberg, Great Karoo, South Africa. Catena, 50, 165-184.

Buol S. W., Hole F. D. McCracken, R.J., 1994. Soil Genesis and Classification. Iowa State University Press. Ames.

Cyr A.J., Gramger D.E., 2008. Dynamic equilibrium among erosion, river incision, and coastal uplift in the northern and central Apennines, Italy. Geology, 36 (2); 103–106; doi: 10.1130/G24003A.1

Conforti M., Aucelli P.P.C., Robustelli G., Scarmiglia F., 2011. Nat hazards, 56, 881-898.

Dunne T., 1978. Field studies of hillslope flow processes and their significance, in Hillslope Hydrology, edited by M. J.Kirkby, Wiley-Interscience, New York, pp. 227-293.

Eshel G., Levy G.J., Mingelgrin U., Singer M.J., 2004. Critical evaluation of the use of laser diffraction for particle-size distribution analysis. Soil Sci. Soc. Am. J., 68, 736-743.

Farabegoli E., Rossi P., Costantini B., Gardi C., 1994. Cartografia tematica per lo studio dell'erosione a scala di bacino. Riv. Agron. 28, 371-383.

Freeze R. A., 1971. Three-dimensional, transient, saturated-unsaturated flow in a groundwater basin, Water Resour. Res., 7, 347-366.

Gallart F., Llorens P., Latron J., Regüés D., 2002. Hydrological processes and their seasonal controls in a small Mediterranean mountain catchment in the Pyrenees. Hydrology and Earth System Sciences 6, 527-537.

Gallart F., Balasch J.C., Regüés D., Soler M., Castelltort X., 2005a. Catchemnt dynamics in a Mediterranean mountain environment: the Vallcebre research basins (southeastern Pyrenees). Developments in Earth Surface processes, 7:17-29.

Gallart F., Balasch C., Regüés D., Soler M., 2005b. Catchment dynamics in a Mediterranean mountain environment: the Vallcebre research basins (South Eastern Pyrenees). II: Temporal and spatial dynamics of erosion and stream sediment transport. In: Garcia, C., Batalla, R. (Eds.), Catchment Dynamics and River Processes: Mediterranean and other Climate Regions. Elsevier, Amsterdam.

Garcia-Ruiz J.M., Arnaez, J., Begueria, S., Seeger M., Marti-Bono, C., Regues D., Lana-Renault, N., White S., 2005. Flow generation in an intensively disturbed abandoned farmland catchment, Central Spanish Pyrenees. Catena, 59: 79-92.

Gardi C., 2001. Land use, agronomic management and water quality in a small Northern Italian watershed. Agriculture, ecosystes, environment, 87(1): 1-12.

Heng B.C.P., Sander G.C., Armstrong A., Quinton J.N., Chandler J.H. and Scott C.F., 2011. Modeling the dynamics of soil erosion and size-selective sediment transport over nonuniform topography in flume-scale experiments. Water Resources research, 47(2):1-11.

Horton R.E., 1933. The role of infiltration in the hydrologic cycle. Transaction American Geophysical Unini 14: 446-460.

Lana-Renault, N., Regüés, D., 2009. Seasonal patterns of suspended sediment transport in an abandoned farmland catchment in the central Spanish Pyrenees. Earth Surface Processes and Landforms 34, 1291-1301.

Latron J., Soler M., Llorens P., Gallart F., 2008. Spatial and temporal variability of the hydrological response in a small Mediterranean research catchment (Vallcebre, Eastern Pyrenees). Hydrological Processes 22, 775-787.

López-Tarazón J.A., Batalla R.J., Vericat D., Balasch

J.C., 2010. Rainfall, flowand sediment tranport relations in a mesoscale mountainous catchment: The River Isabena (Ebro basin). Catena, 82: 23-24.

Martnez-Mena, M., Albaladejo, J., Castillo, V.M., 1998. Factors influencing surface runoff generation in a Mediterranean semi-arid environment: Chicamo watershed, SE Spain. Hydrological Processes 12, 741-754.

Marquardt D.W., 1963. An algorithm for least-squares estimation of non-linear parameters. J. Soc. Ind. Appl. Math. 11, 431-441.

Miller W.P. and Baharuddin M.K., 1987. Particle size of interrill-eroded sediments from highly weathered soils. Soil Science Society of America Journal, 51, 1610-1615.

Morbidelli R., Corradini C., Saltalippi C., Brocca L., 2012. Initial soil water content as input to field-scale infiltration and surface runoff models. Water Resources Management, 26(7), 1793-1807, doi: 10.1007/s11269-012-9986-3. http://dx.doi.org/10.1007/s11269-012-9986-3

Nadal-Romero E., Latron J., Martí-Bono C., Regüés, D., 2008. Temporal distribution of suspended sediment transport in a humid Mediterranean badland area: the Araguás catchment, Central Pyrenees. Geomorphology 97, 601-616.

Nearing M.A., Jetten V., Baffaut C., Cerdan O., Couturier A., Hernandez M., Le Bissonnais Y., Nichols M.H., Nunes J.P., Renschler C.S., Souchere V., van Oost K., 2005. Modeling response of soil erosion and flow to changes in precipitation and cover. Catena, 61, 23.

Nu-Fang F., Zhi-Hua S., Lu L., Cheng J., 2011. Rainfall, runoff and suspended sediment delivery relationships in a small agricultural watershed of the Three Gorges area, China. Geomorphology, 135, 158-166.

Ongley E.D., Bynoe M.C., Perciva J.B., 1981. Physical and geochemical characteristics of suspended solids. Wilton Creek, Ontario. Canadian Journal of Earth Science, 18, 1365-1379.

Parsons A.J., Stone P.M., 2006. Effects of intra-storm variations in rainfall intensity on interill flow and erosion. Catena, 67, 68-78.

Phillips, J.M., Walling, D.E., 1995. Measurement in situ of the effective particle-size characteristics of fluvial suspended sediment by means of a field-portable laser backscatter probe: some preliminary results. Mar. Freshwat. Res., 46:349-357.

Piccarreta M., Capolongo D., Boenzi F., Bentivenga M., 2006. Implication of decadal changes in precipitation and land use policy to soil erosion in Basilicata, Italy. Catena, 65, 138-151.

Pieri L., Bittelli M., Rossi P., 2006. Laser diffraction, trasmission electron microscopy and image analysis to evaluate a bimodal Gaussian model for particle size distribution in soils. Geoderma, 135C, 118-132.

Pieri L., Poggio M., Vignudelli M., Bittelli M., 2014. Evaluation of the WEPP model and digital elevation grid size, for simulation of stream flow and sediment yield in a heterogeneous catchment. Earth Surface Processes and Landforms. doi. 10.1002/esp.3527. ISSN: 1096-9837.

Piñol J., Beven K., Freer J., 1997. Modelling the hydrological response of Mediterranean catchments, Prades Catalonia. The use of distributed models as aid to hypothesis formation. Hydrological process, 11, 1287-1306.

Proffitt A.P.B., Rose C.W., 1991. Soil erosion processes. I. The relative importance of rainfall detachment and flowentrainment. Aust. J. Soil Res., 29, 671-683.

Selby M.J. 1982. Hillslope materials and processes. Oxford University press. 264 pp.

Soler M., Latron J., Gallart F., 2008. Relationships between suspended sediment concentrations and flow in two small in two small research basins in a mountainous Mediterranean area (Vallcebre, Eastern Pyrennes). Geomorpholy, 98: 143-152.

Young R.A., 1980. Characteristics of eroded sediment. Trans. ASAE, 23, 1139-1142.

Walling D.E., Moorehead, P.W., 1989. The particle size characteristics of fluvial suspended sediment: an overview. Hydrobiologia, 176/177, 125-149.

Walling D.E., 1996. Suspended sediment transport by rivers: a gemorphological and hydrological perspective. Arch. Hydrobiol., 47,1-27.

Walling D.E.,. Owens P.N, Waterfall B.D., Leeks G. J.L., Wass P.D., 2000. The particle size characteristics of fluvial suspended sediment in the Humber and Tweed catchments, UK. The science of the total environment, 525, 205-222.

Warner R. M., 2012. Applied Statistics: From Bivariate Through Multivariate Techniques. Sage Publications (CA) 1172 p.

Wischmeier WH, Smith D.D., 1978. Predicting rainfall erosion losses. A guide to conservation planning. US Dept. Agric. Agricultural Handbook, USDA: Blacksburg, VA; 537.